Supplementary Information

Development of liquid-crystalline smectic nanoporous membranes for the removal of SARS-CoV-2 and waterborne viruses

Takeshi Sakamoto,*[a] Kazuhiro Asakura,[a] Naru Kang,[a] Riki Kato,[a] Miaomiao Liu,[b] Tsuyoshi Hayashi,[c] Hiroyuki Katayama*[b,d] and Takashi Kato*[a,d,e]

[a] Department of Chemistry and Biotechnology, School of Engineering, The University of Tokyo, Bunkyo-ku, Tokyo 113-8656, Japan
E-mail: t_saka@chembio.t.u-tokyo.ac.jp
E-mail: kato@chiral.t.u-tokyo.ac.jp

[b] Department of Urban Engineering, School of Engineering, The University of Tokyo, Bunkyo-ku, Tokyo 113-8656, Japan
E-mail: katayama@env.t.u-tokyo.ac.jp

[c] Department of Virology II, National Institute of Infectious Diseases, Musashi-Murayama, Tokyo 208-0011, Japan

[d] Research Center for Water Environment Technology, School of Engineering, The University of Tokyo, Bunkyo-ku, Tokyo 113-8656, Japan

[e] Research Initiative for Supra-Materials, Shinshu University, Wakasato, Nagano 380-8553, Japan

Contents

1. Details of compound synthesis

All reagents were purchased from Sigma-Aldrich Japan (Tokyo, Japan), Kanto Chemical (Tokyo, Japan), TCI (Tokyo, Japan) and FUJIFILM Wako Pure Chemical (Osaka, Japan) and were used as received. Unless otherwise noted, all reactions were performed under argon atmosphere in a dry solvent purchased from Kanto Chemical. Compounds **1** and **2** were synthesized following the synthetic routes shown in **Schemes S1** and **S2**, respectively. The details are provided in the subsections below.

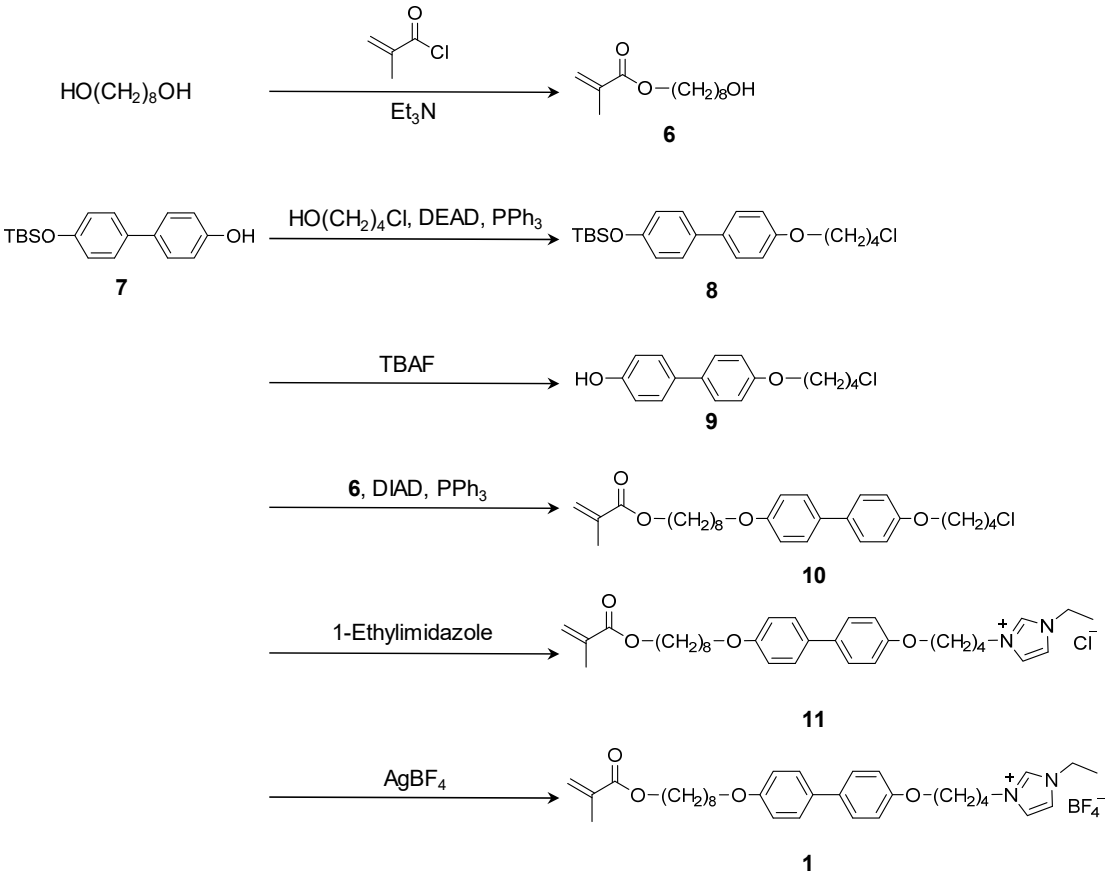

Scheme S1. Synthesis of compound **1**.

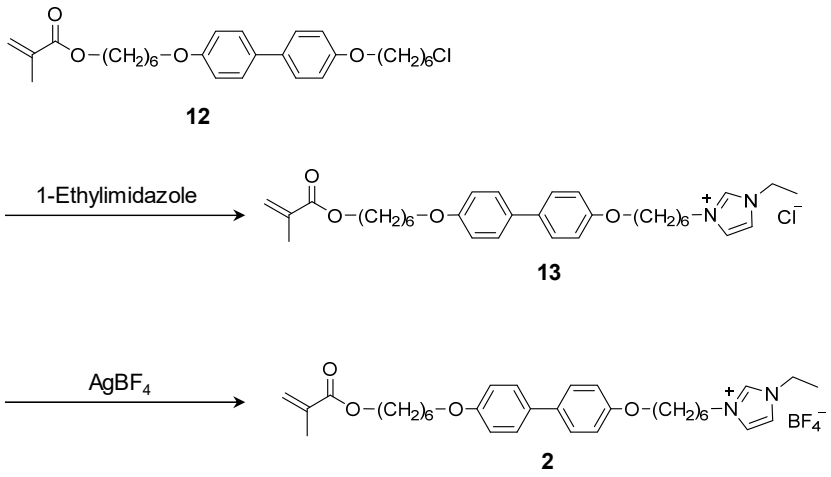

Scheme S2. Synthesis of compound **2**.

8-Hydroxyoctyl methacrylate (**6**)

1,8-Octanediol (5.84 g, 39.9 mmol) and triethylamine (4.04 g, 40.0 mmol) were dissolved in tetrahydrofuran (THF) (30 mL) and cooled to 0 °C. Methacryloyl chloride (2.11 g, 20.2 mmol) dissolved in THF (30 mL) was added dropwise through a dropping funnel. The reaction mixture was stirred for 30 min at 0 °C and then gradually warmed to room temperature. After stirring in the dark for 22 h, the reaction mixture was diluted with water and extracted three times with ethyl acetate. The organic layer was then washed with water and dried over $MgSO_4$. After filtration and concentration in vacuo, the crude product was purified using silica gel column chromatography (eluent: gradient of CH_2Cl_2/ethyl acetate = 98/2 to 90/10) to obtain a colorless oil of 8-hydroxyoctyl methacrylate **6** (1.90 g, 8.86 mmol, 44%).

^{1}H NMR (400 MHz): δ = 6.11–6.08 (m, 1H), 5.56–5.54 (m, 1H), 4.14 (t, J = 6.6 Hz, 2H), 3.64 (t, J = 6.6 Hz, 2H), 1.95 (s, 3H), 1.71–1.52 (m, 4H) and 1.45–1.30 (m, 8H).

^{13}C NMR (100 MHz): δ = 167.64, 136.53, 125.24, 64.83, 62.84, 32.72, 29.32, 29.22, 28.60, 25.92, 25.69 and 18.32.

4-*tert*-Butyldimethylsilyloxy-4′-(4-chlorobutyloxy)-1,1′-biphenyl (**8**)

Compound **7**[1] (7.30 g, 24.3 mmol) and triphenylphosphine (7.78 g, 29.7 mmol) were dissolved in toluene (40 mL), and 4-chloro-1-butanol (3.43 g, 31.6 mmol) was added. To this solution, diethyl azocarboxylate solution in toluene (12.9 g, approximately 2.2 M) was added dropwise through a dropping funnel. The reaction mixture was stirred for 3 d at room temperature. The reaction mixture was diluted with a saturated NH_4Cl aqueous solution and extracted four times with ethyl acetate. The organic layer was then washed with brine and dried over $MgSO_4$. After filtration and concentration in vacuo, the crude

product was purified using silica gel column chromatography (eluent: hexane/ethyl acetate = 95/5) to obtain a white solid of 4-*tert*-butyldimethylsilyloxy-4′-(4-chlorobutyloxy)-1,1′-biphenyl **8** (7.75 g, 19.8 mmol, 82%).
^{1}H NMR (400 MHz): δ = 7.46 (d, J = 8.8 Hz, 2H), 7.40 (d, J = 8.8 Hz, 2H), 6.93 (d, J = 8.8 Hz, 2H), 6.88 (d, J = 8.8 Hz, 2H), 4.03 (t, J = 6.0 Hz, 2H), 3.64 (t, J = 6.2 Hz, 2H), 2.05–1.92 (m, 4H), 1.00 (s, 9H) and 0.22 (s, 6H).
^{13}C NMR (100 MHz): δ = 157.94, 154.76, 133.92, 133.59, 127.73, 127.62, 120.28, 114.65, 67.00, 44.79, 29.33, 26.69, 25.70, 18.23 and –4.39.
Elemental analysis calculated (%) for $C_{22}H_{31}ClO_2Si$: C, 67.58; H, 7.99. Found: C, 67.55; H, 8.05.

4-(4-Chlorobutyloxy)-4′-hydroxy-1,1′-biphenyl (**9**)
Compound **8** (4.53 g, 11.6 mmol) was dissolved in THF (40 mL), and tetrabutylammonium fluoride solution was added to THF (13.9 mL, approximately 1 M). The reaction mixture was stirred at room temperature for 18 h. The reaction mixture was then diluted with an HCl aqueous solution and extracted three times with ethyl acetate. The organic layer was then washed with water and dried over $MgSO_4$. After filtration and concentration in vacuo, a white solid of 4-(4-chlorobutyloxy)-4′-hydroxy-1,1′-biphenyl **9** (3.38 g, 12.2 mmol) was obtained. The reaction proceeded quantitatively.
^{1}H NMR (400 MHz): δ = 7.45 (d, J = 8.8 Hz, 2H), 7.43 (d, J = 8.8 Hz, 2H), 6.94 (d, J = 8.8 Hz, 2H), 6.88 (d, J = 8.8 Hz, 2H), 4.70 (s, 1H), 4.03 (t, J = 6.0 Hz, 2H), 3.64 (t, J = 6.4 Hz, 2H) and 2.06–1.92 (m, 4H).
^{13}C NMR (100 MHz): δ = 158.02, 154.61, 133.71, 133.49, 127.96, 127.73, 115.60, 114.73, 67.07, 44.78, 29.35 and 26.71.
Elemental analysis calculated (%) for $C_{16}H_{17}ClO_2$: C, 69.44; H, 6.19. Found: C, 69.44; H, 6.14.

8-((4′-(4-Chlorobutoxy)-[1,1′-biphenyl]-4-yl)oxy)octyl methacrylate (**10**)
Compound **9** (2.50 g, 9.06 mmol), triphenylphosphine (2.86 g, 10.9 mmol) and compound **6** (1.98 g, 9.24 mmol) were dissolved in THF (50 mL) and cooled to 0 °C. Diisopropyl azocarboxylate (2.20 g, 10.9 mmol) was added dropwise at the same temperature, and the reaction mixture was stirred at room temperature in the dark for 20 h. The reaction mixture was diluted with water and extracted three times with ethyl acetate. The organic layer was then washed with brine and dried over $MgSO_4$. After filtration and concentration in vacuo, the crude product was purified using silica gel

column chromatography (eluent: gradient of hexane/CH_2Cl_2 = 90/10 to 70/30) to obtain a white solid of 8-((4′-(4-chlorobutoxy)-[1,1′-biphenyl]-4-yl)oxy)octyl methacrylate **10** (3.03 g, 6.41 mmol, 71%).

^{1}H NMR (400 MHz): δ = 7.46 (d, J = 9.2 Hz, 4H), 6.94 (d, J = 9.0 Hz, 4H), 6.11–6.09 (m, 1H), 5.56–5.53 (m, 1H), 4.14 (t, J = 6.6 Hz, 2H), 4.03 (t, J = 5.8 Hz, 2H), 3.98 (t, J = 6.6 Hz, 2H), 3.64 (t, J = 6.4 Hz, 2H), 2.05–1.92 (m, 7H), 1.84–1.64 (m, 4H) and 1.52–1.33 (m, 8H).

^{13}C NMR (100 MHz): δ = 167.57, 158.26, 157.95, 136.57, 133.63, 133.26, 127.71, 127.68, 125.16, 114.75, 114.72, 68.02, 67.05, 64.79, 44.78, 29.35, 29.27, 29.19, 28.61, 26.71, 25.99, 25.93 and 18.35.

Elemental analysis calculated (%) for $C_{28}H_{37}ClO_4$: C, 71.09; H, 7.88. Found: C, 71.05; H, 7.80.

1-Ethyl-3-(4-((4'-((8-(methacryloyloxy)octyl)oxy)-[1,1'-biphenyl]-4-yl)oxy)butyl)-imidazolium chloride (**11**)

Compound **10** (1.51 g, 3.19 mmol) and a polymerization inhibitor (2,6-di-*tert*-butylphenol (340 mg, 1.65 mmol)) were added to 1-ethylimidazole (10 mL, 104 mmol) and stirred at 55 °C for 32 h in the dark. The reaction mixture was then purified using silica gel column chromatography (eluent: CH_2Cl_2/MeOH = 90/10) to obtain a white solid of 1-ethyl-3-(4-((4'-((8-(methacryloyloxy)octyl)oxy)-[1,1'-biphenyl]-4-yl)oxy)butyl)-imidazolium chloride **11** (1.46 g, 2.56 mmol, 80%).

^{1}H NMR (400 MHz): δ = 11.17 (s, 1H), 7.48–7.42 (m, 4H), 7.28 (d, J = 17.6 Hz, 2H), 6.96–6.89 (m, 4H), 6.11–6.09 (m, 1H), 5.56–5.53 (m, 1H), 4.50 (t, J = 7.2 Hz, 2H), 4.41 (q, J = 7.5 Hz, 2H), 4.14 (t, J = 6.8 Hz, 2H), 4.06 (t, J = 6.0 Hz, 2H), 3.98 (t, J = 6.4 Hz, 2H), 2.24–2.14 (m, 2H), 1.94 (s, 3H), 1.93–1.86 (m, 2H), 1.83–1.75 (m, 4H), 1.73–1.63 (m, 2H), 1.60 (t, J = 7.6 Hz, 3H) and 1.53–1.33 (m, 8H).

1-Ethyl-3-(4-((4'-((8-(methacryloyloxy)octyl)oxy)-[1,1'-biphenyl]-4-yl)oxy)butyl)-imidazolium tetrafluoroborate (**1**)

Compound **11** (456 mg, 0.80 mmol) and $AgBF_4$ (516 mg, 2.65 mmol) were added to EtOH (25 mL). The reaction mixture was then stirred at room temperature for 22 h in the dark. The insoluble silver salt solid was filtered with celite, and the filtrate was concentrated in vacuo, followed by purification using silica gel column chromatography (eluent: CH_2Cl_2/MeOH = 90/10) to obtain a white solid of 1-ethyl-3-(4-((4'-((8-(methacryloyloxy)octyl)oxy)-[1,1'-biphenyl]-4-yl)oxy)butyl)-imidazolium tetrafluoroborate **1** (506 mg, 0.82 mmol). The reaction was performed under

atmospheric condition using normal EtOH and proceeded quantitatively.
^{1}H NMR (400 MHz): δ = 8.98 (s, 1H), 7.47–7.42 (m, 4H), 7.28 (d, J = 17.2 Hz, 2H), 6.96–6.86 (m, 4H), 6.11–6.09 (m, 1H), 5.56–5.53 (m, 1H), 4.32 (t, J = 7.4 Hz, 2H), 4.25 (q, J = 7.5 Hz, 2H), 4.14 (t, J = 6.8 Hz, 2H), 4.03 (t, J = 6.0 Hz, 2H), 3.98 (t, J = 6.8 Hz, 2H), 2.17–2.07 (m, 2H), 1.94 (s, 3H), 1.89–1.75 (m, 4H), 1.72–1.64 (m, 2H), 1.54 (t, J = 7.6 Hz, 3H) and 1.52–1.34 (m, 8H).
^{13}C NMR (100 MHz): δ = 158.33, 157.64, 136.57, 136.21, 133.81, 127.74, 127.65, 125.18, 122.03, 121.50, 114.80, 114.72, 68.04, 66.98, 64.79, 49.96, 45.43, 29.28, 29.19, 28.61, 26.00, 25.94, 18.35 and 15.12.
Elemental analysis calculated (%) for $C_{33}H_{45}BF_4N_2O_4$: C, 63.87; H, 7.31; N, 4.51. Found: C, 63.96; H,7.21; N, 4.59.
MS (MALDI-TOF): calculated for $[M\text{-}BF_4]^+$, 533.34. Found: 533.28.

1-Ethyl-3-(6-((4'-((6-(methacryloyloxy)hexyl)oxy)-[1,1'-biphenyl]-4-yl)oxy)hexyl)-imidazolium chloride (13)

Compound **12**[2] (1.0 g, 2.1 mmol) and 2,6-di-*tert*-butylphenol (200 mg, 0.97 mmol) were added to 1-ethylimidazole (10 mL, 118 mmol) and stirred at 55 °C for 48 h in the dark. The reaction mixture was diluted with water and extracted three times with CH_2Cl_2. The organic layer was then washed with brine and dried over $MgSO_4$. After filtration and concentration in vacuo, the crude product was purified using silica gel column chromatography (eluent: CH_2Cl_2/MeOH = 84/16) to obtain 1-ethyl-3-(6-((4'-((6-(methacryloyloxy)hexyl)oxy)-[1,1'-biphenyl]-4-yl)oxy)hexyl)-imidazolium chloride **13** (0.42 g, 0.74 mmol, 37%).
^{1}H NMR (400 MHz): δ = 11.31 (s, 1H), 7.49–7.39 (m, 4H), 7.16–7.08 (m, 2H), 6.97–6.88 (m, 4H), 6.09 (s, 1H), 5.56–5.53 (m, 1H), 4.47–4.32 (m, 4H), 4.15 (t, J = 6.6 Hz, 2H), 3.98 (t, J = 6.4 Hz, 4H), 2.02–1.94 (m, 2H), 2.02–1.93 (s, 3H), 1.83–1.75 (m, 4H), 1.74–1.65 (m, 2H), 1.60 (t, J = 7.6 Hz, 3H) and 1.53–1.39 (m, 8H).

1-Ethyl-3-(6-((4'-((6-(methacryloyloxy)hexyl)oxy)-[1,1'-biphenyl]-4-yl)oxy)hexyl)-imidazolium tetrafluoroborate (2)

Compound **13** (0.37 g, 0.65 mmol) and $AgBF_4$ (0.15 g, 1.57 mmol) were added to EtOH (15 mL). This reaction was performed under atmospheric condition using normal EtOH. The reaction mixture was then stirred at 0 °C for 2 h. The insoluble silver salt solid was

filtered with celite, and the filtrate was concentrated in vacuo. The crude product was purified using silica gel column chromatography (eluent: CH_2Cl_2/MeOH = 70/30) to obtain 1-ethyl-3-(6-((4'-((6-(methacryloyloxy)hexyl)oxy)-[1,1'-biphenyl]-4-yl)oxy)hexyl)-imidazolium tetrafluoroborate **2** (260 mg, 0.42 mmol, 65%).

^{1}H NMR (400 MHz): δ = 9.11 (s, 1H), 7.49–7.39 (m, 4H), 7.16–7.08 (m, 2H), 6.97–6.88 (m, 4H), 6.09 (s, 1H), 5.55–5.52 (m, 1H), 4.47–4.32 (m, 4H), 4.15 (t, J = 6.6 Hz, 2H), 3.98 (t, J = 6.6 Hz, 4H), 2.01–1.91 (m, 5H), 1.84–1.75 (m, 4H), 1.74–1.63 (m, 2H), 1.57 (t, J = 7.6 Hz, 3H) and 1.53–1.39 (m, 8H).

^{13}C NMR (100 MHz): δ = 167.64, 158.27, 158.13, 136.58, 135.97, 133.46, 133.32, 127.75, 127.71, 125.34, 122.10, 121.75, 114.83, 77.11, 67.94, 67.67, 64.75, 50.13, 45.42, 30.05, 29.29, 28.98, 28.65, 25.91, 25.48, 18.43 and 15.24.

Elemental analysis calculated (%) for $C_{33}H_{44}BF_4N_2O_4$: C, 63.87; H, 7.31; N, 4.51. Found: C, 63.94; H, 7.28; N, 4.66.

MS (MALDI-TOF): calculated for $[M\text{-}BF_4]^+$, 533.34. Found: 533.06

2. DSC curves of compounds 1 and 2

(a)

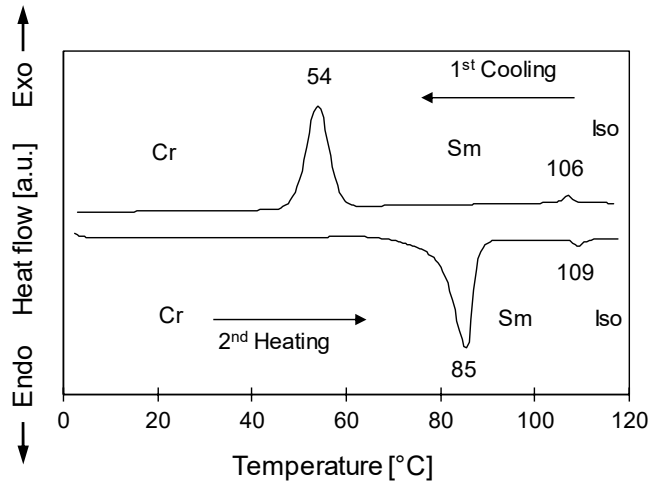

(b)

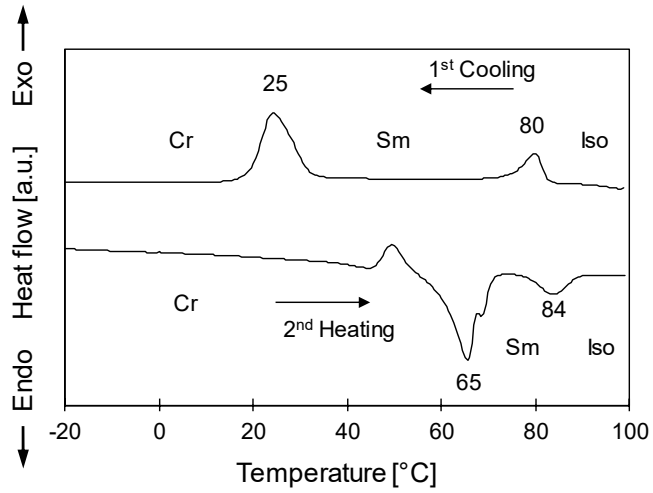

Figure S1. DSC curves of compounds (a) **1** and (b) **2**.

3. Assembled molecular structures of compound 1 (*n* =8, *m* =4)

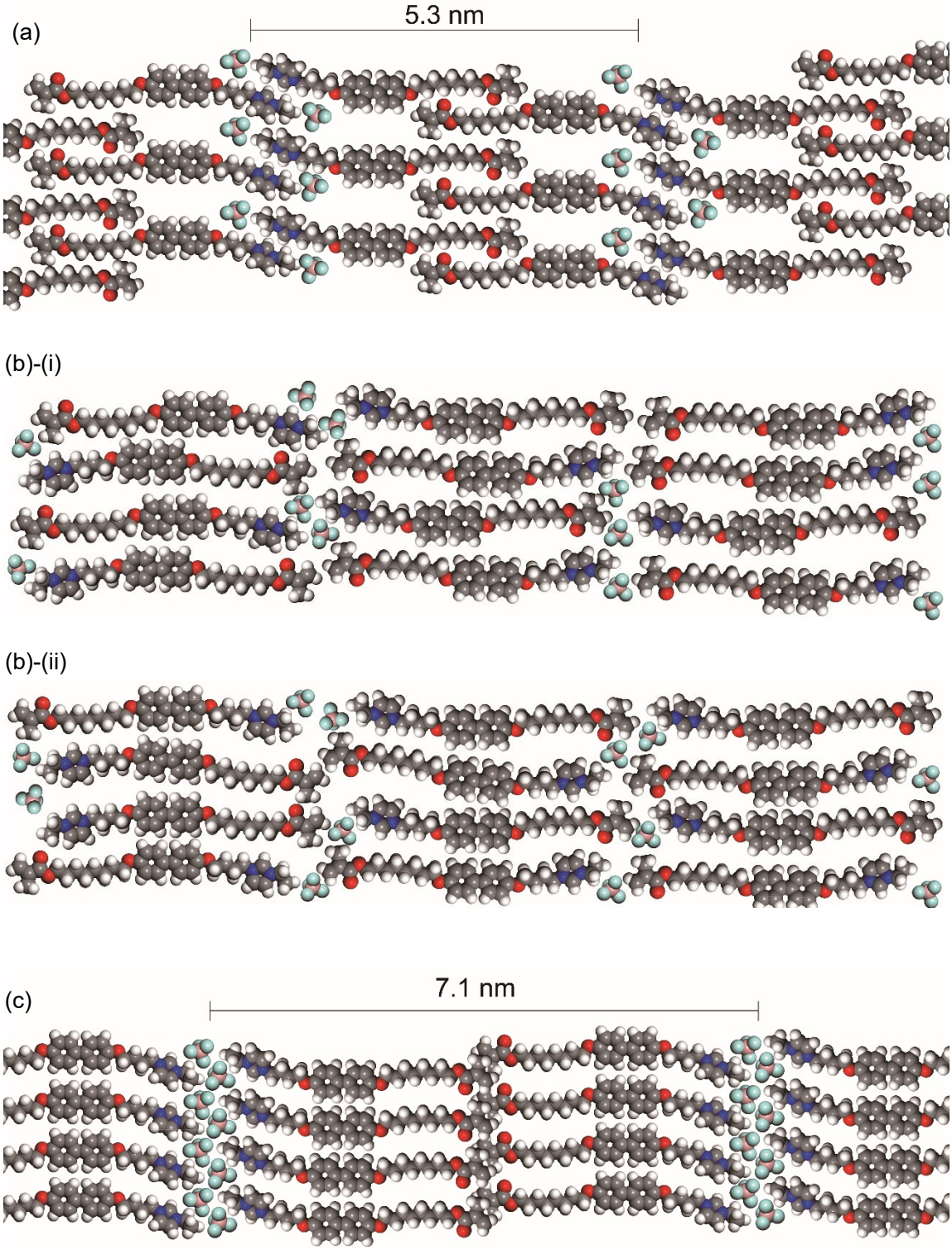

Figure S2. Plausible assembled molecular structures of compound **1** having the alkylene spacers of different lengths (*n* = 8, *m* = 4) on the biphenyl core. (a) Semi-bilayer SmA (SmA_d) structure with a layer spacing of approximately 5.3 nm observed

for the monomer LC state. (b) Virtual monolayer (SmA_1) structures not observed in this study: (i) a structure with aligned terminals of the molecules, (b) a structure with aligned cores of the molecules. (c) Bilayer structure with a layer spacing of approximately 7.1 nm observed for polymerized **1** (**P1**).

4. Structural analysis of compound 2 and P2

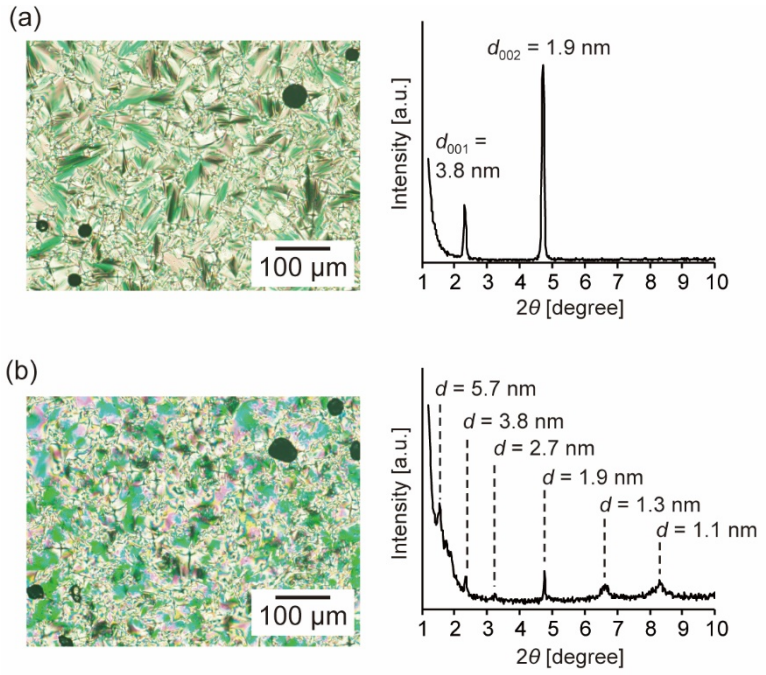

Figure S3. Polarizing optical microscopy (POM) images and X-ray diffraction (XRD) patterns of compound **2** and **P2** in their SmA phases. (a) POM image (left) and XRD pattern (right) of compound **2** at 60 °C. (b) POM image (left) and XRD pattern (right) of **P2** at 60 °C.

5. Assembled molecular structures of compound 2 (*n* = 6, *m* = 6)

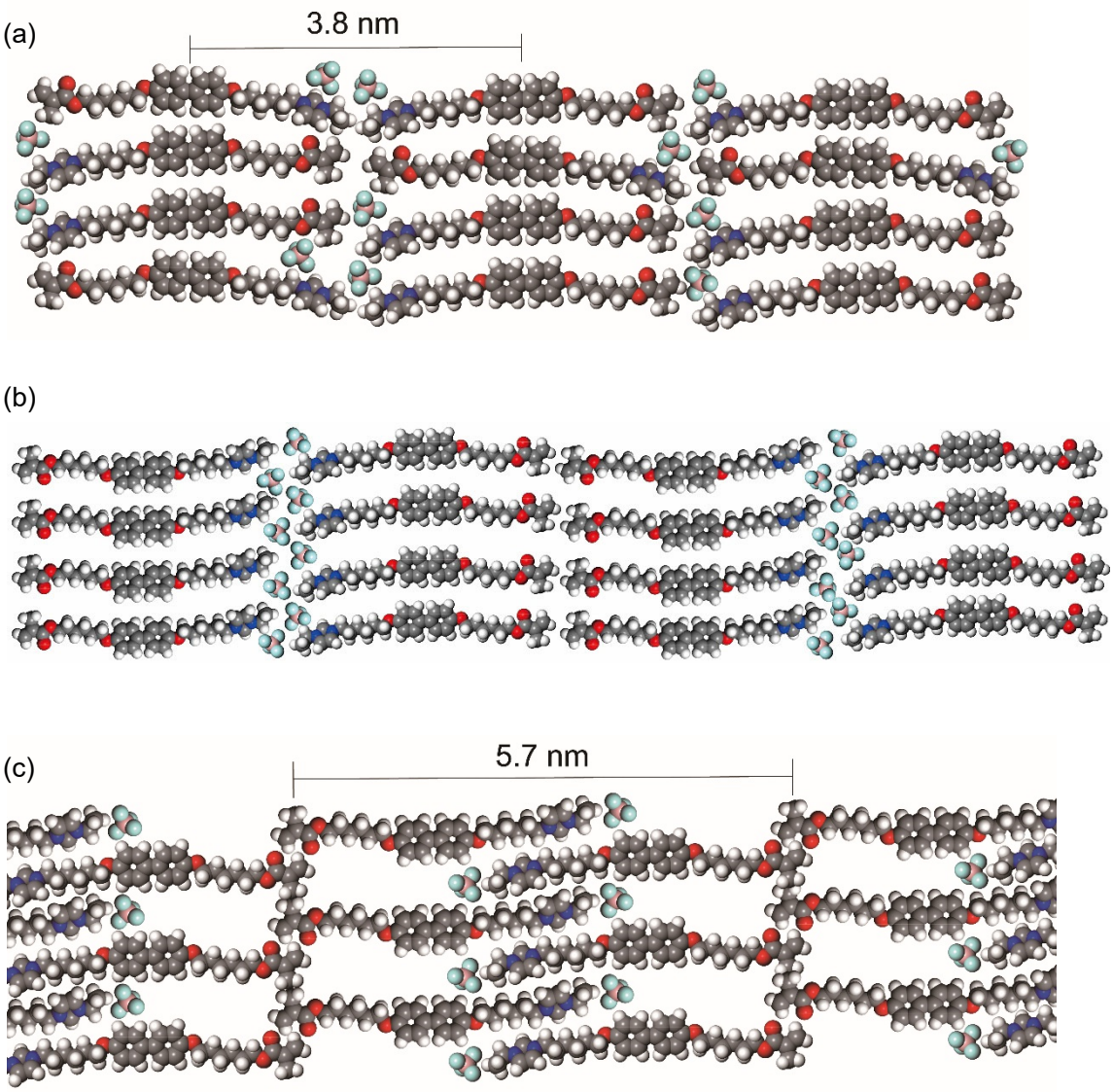

Figure S4. Plausible assembled molecular structures of compound **2** having the alkylene spacers of the same length (*n*, *m* = 6) on both sides of the biphenyl core. (a) Monolayer SmA (SmA_1) structure with a layer spacing of approximately 3.8 nm observed for the monomer LC state. (b) A virtual bilayer (SmA_2) structure not observed in this study. (c) A semi-bilayer structure with a layer spacing of approximately 5.7 nm observed for **P2**.

Supplementary note 1

Compounds **1**–**4** comprise a biphenyl core, a polymerizable methacrylate group and an imidazolium moiety, which are connected by alkylene spacers (**Fig. 2**). For these

compounds, aggregation of the hydrophilic imidazolium moieties induces bilayer (**Fig. 3** type 1) and semi-bilayer structures (**Fig. 3** type 2), in which the hydrophilic parts and hydrophobic parts are segregated in nanometre scale compared to monolayer structures (**Fig. 3** type 3). In contrast, the assembled molecular structures induced by the aggregation of the hydrophobic parts consisting of a rigid core and alkyl chains are expected to be affected by symmetry of the hydrophobic parts. The hydrophobic parts with symmetric alkyl chains on both sides of the rigid core are easy to stack in both of monolayer (**Fig. S4a**) and bilayer structures (**Fig. S4b**). However, asymmetric hydrophobic parts disturb assembly of the core and the alkyl chains in monolayer structures (**Fig. S2b**). Then, compounds **2** and **3** having the symmetrical spacers formed SmA_1 phases and compounds **1** and **4** formed semi-bilayer (SmA_d) phases. In addition, in the SmA_d structures of **1**, both of the interaction of the ionic moieties and hydrophobic parts contribute to the formation of assembled structures, and thus, the isotropization temperature of **1** was higher than those of **2** and **3**.

Supplementary note 2

The XRD patterns of **1** (**Fig. 4a** right) and **P1** (**Fig. 4b** right) suggest that periodic structures were formed during the photopolymerization of **1**. For compound **2**, periodic structures during the polymerization were also formed (**Fig. S3a** right and **S3b** right). However, the POM images show little change during the photopolymerization, especially for compound **1** (**Fig**. **4a** left and **4b** left). These results indicate that the assembled molecular structures of **1**, such as orientation and domains were almost maintained.

Differences between the POM images of **2** (**Fig. S3a** left) and **P2** (**Fig. S3b** left) were more noticeable than those of **1** (**Fig**. **4a** left) and **P1** (**Fig**. **4b** left). These results suggest that polymerization of **2** induced more changes in the assembled molecular structures compared to **1**. However, water flux through **P2** membrane was lower than that through **P1** membrane and these membranes showed similar high virus rejection (**Fig. 6**). Then, the pinhole-free surface and ordered structures were expected to be almost maintained during the polymerization of **2**.

6. Details for the photopolymerization and characterization of P1

Photopolymerization of polymer films for structural analyses:

Polymer film**s** for the POM, TG, DSC and FTIR analyses were prepared as follows: The monomer and the photoinitiator 2,2-dimethoxy-2-phenylacetophenone (1 wt.%) were sandwiched between PVA-coated glasses and heated to 100 °C and then maintained or cooled to the desired temperature (100 °C for **1** and 60°C for **2**). After that, the film mixtures were irradiated with UV light (365 nm, 30 mW cm^{-2}) using a UV-LED system for 20 min in their LC states. Self-standing films for TG, DSC and FTIR measurements were prepared by immersing the samples in water after the polymerization. **P1** and **P2** for the XRD measurements were polymerized on glass substates under N_2. The conditions for temperature and UV light were the same as above.

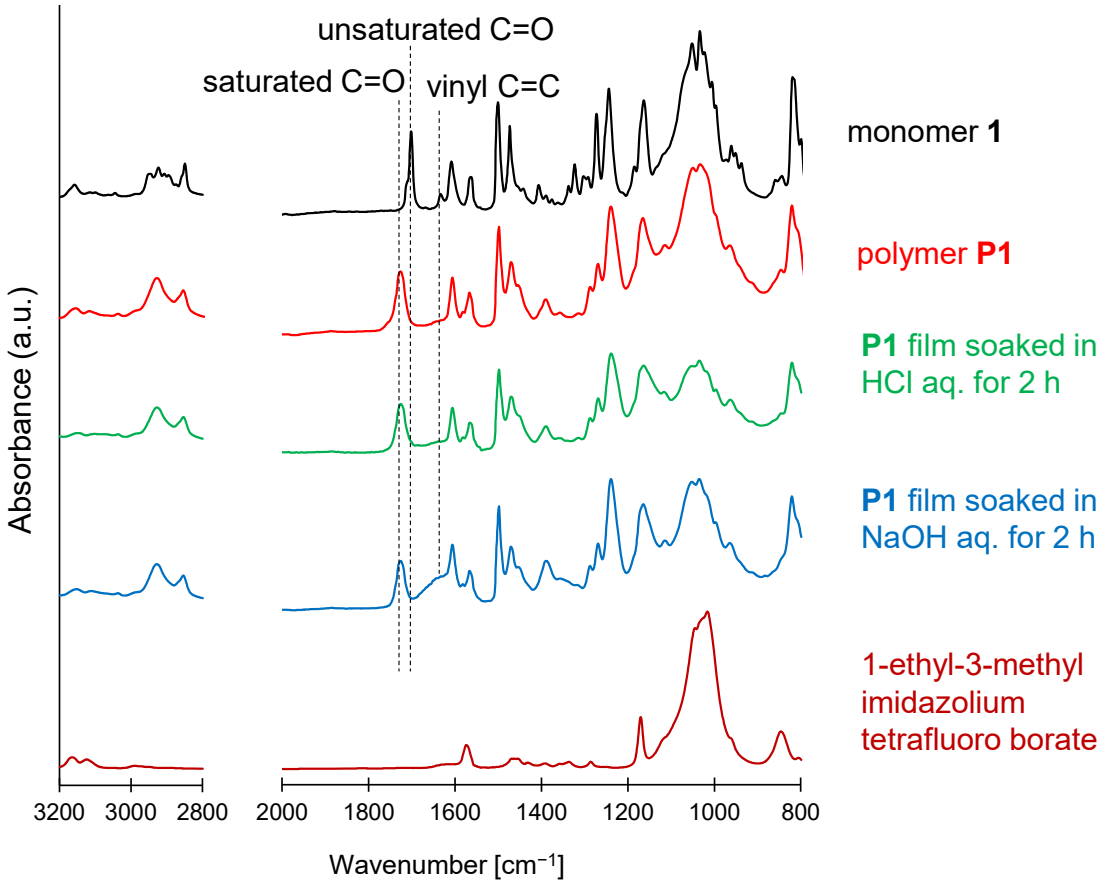

Figure S5. FTIR spectra for compound **1** and **P1**.

Supplementary note 3

The absorbance peaks for the methacrylate moiety of monomer **1** such as unsaturated C=O and vinyl C=C were shifted or disappeared for **P1** (**Fig. S5**). This observation shows that polymerization of the methacrylate moieties was proceeded. The IR spectra for 1-ethyl-3-methyl imidazolium tetrafluoro borate is also shown for comparison in **Fig. S5**.

P1 films were soaked into HCl aq. (pH 1) and NaOH aq. (pH 14) in order to examine their acid and alkali tolerance[3] assuming chemical cleaning operations of water-treatment membranes.

After soaking into the HCl or NaOH aq. solutions, the intensity of absorbance peaks for the ionic moieties of **P1** were reduced, which suggests that **P1** films were hydrolyzed during the soaking processes.

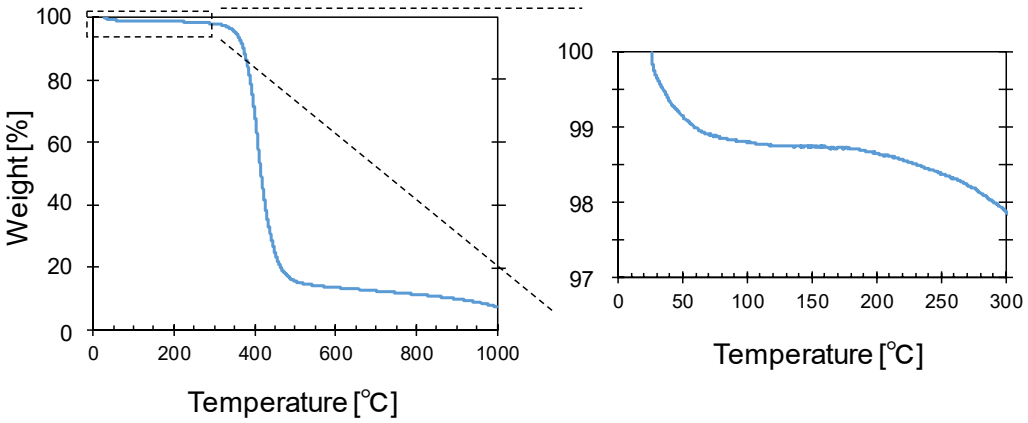

Figure S6. Thermogravimetric (TG) curves for thermal decomposition behavior of **P1**.

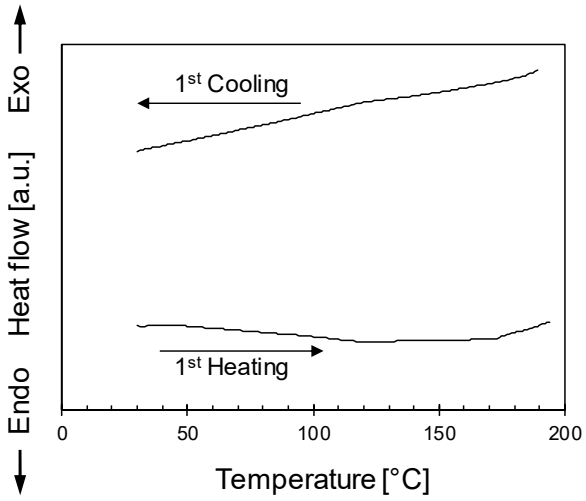

Figure S7. DSC curves of **P1**.

Supplementary note 4

TG measurements were conducted with a TG-8122 (Rigaku) under a flow of N_2 (100 $cm^3\ min^{-1}$) in the temperature range of 25 up to 1000 °C at a heating rate of 10 °C min^{-1} (**Fig. S6**). The weight-loss under 100 °C was because of evaporation of water, which was used to dissolve the PVA layer and adsorbed on the surface of **P1**. On heating, thermal decomposition of **P1** was started at around 170 °C. On the DSC measurements (**Fig. S7**), **P1** did not show any clear phase transition peaks under 170 °C on heating and cooling.

7. Structures of the nanostructured membrane for water-treatment

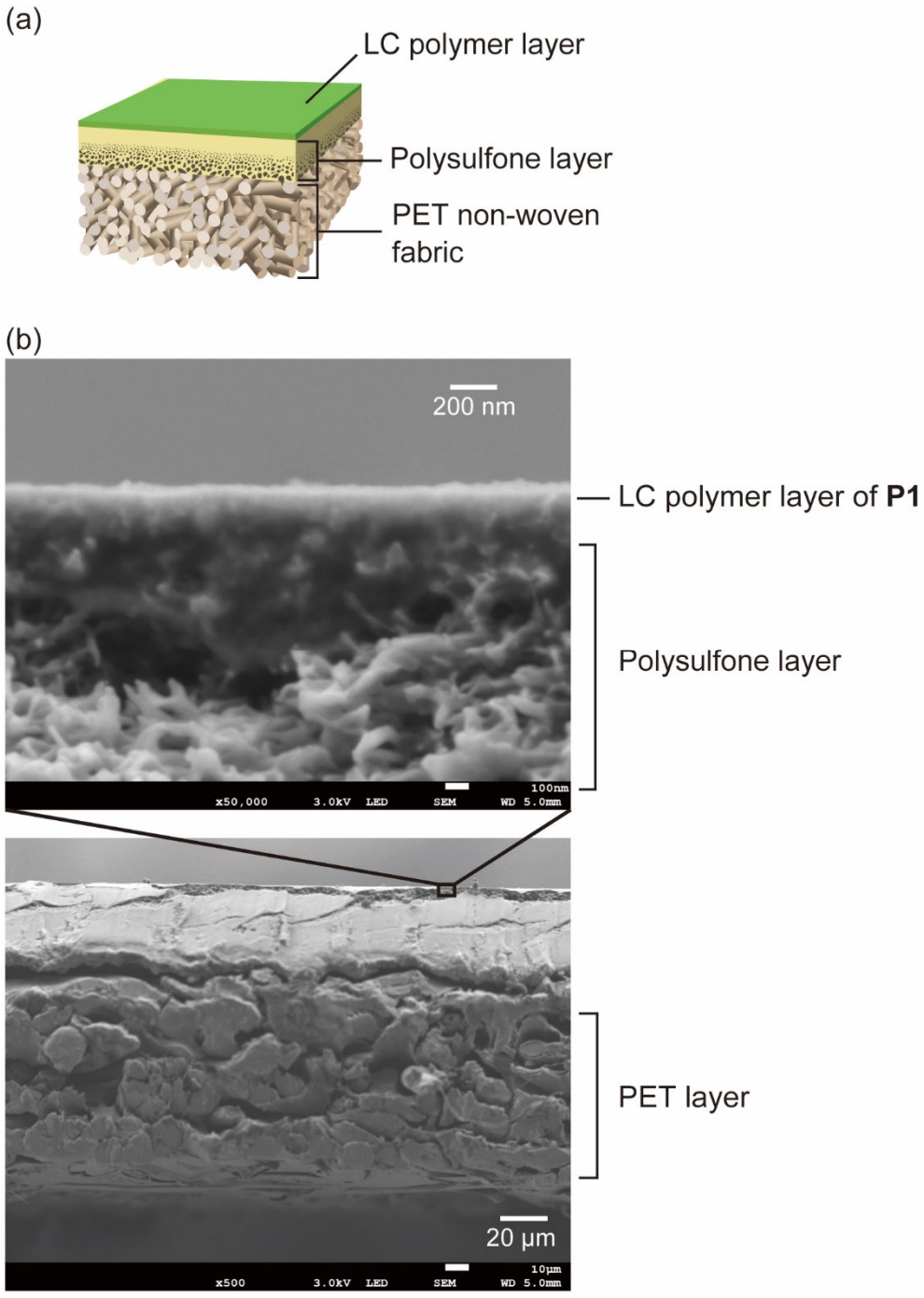

Figure S8. (a) Schematic of the nanostructured membrane based-on the LC polymer and polysulfone substrate. (b) Scanning electron microscopy (SEM) images of cross-section of **P1** membrane.

Supplementary note 5

Cross section of **P1** membrane cut in liquid nitrogen was observed with JSM-

7800FPRIME (JEOL) operated at 3kV. SEM images of the cross-section revealed that dense LC polymer film was on the porous polysulfone layer and that thickness of the LC polymer layer was 100–150 nm. This thickness is similar to that of the LC polymer layer in our previous report.[4]

8. Primers and probes for the PCR

Table S1. Primers and probes for the investigated viruses (Qβ, MHV, AiV and SARS-CoV-2).

	Primer/Probe	Sequences	Ref.
Qβ	VTB4-FphGIII(Qβ)f	CCGTCCGTTGAGGGTATGTT	[5]
	VTB4-FphGIII(Qβ)r	CGAGGSGTACACGCTTG	
	VTB4-FphGIIIprobe	CGGYCATCCGTCCTTCAAGTTTGC	
MHV	MHV-F	GGAACTTCTCGTTGGGCATTATACT	[6]
	MHV-R	ACCACAAGATTATCATTTTCACAACATA	
	MHV-P	ACATGCTACGGCTCGTGTAACCGAACTGT	
AiV	AiV-AB-F	GTCTCCACHGACACYAAYTGGAC	[7]
	AiV-AB-R	GTTGTACATRGCAGCCCAGG	
	AiV-AB-TP	TTYTCCTTYGTGCGTGC	
SARS-CoV-2	2019-nCoV_N1-F	GACCCCAAAATCAGCGAAAT	[8]
	2019-nCoV_N1-R	TCTGGTTACTGCCAGTTGAATCTG	
	2019-nCoV_N1-P	ACCCCGCATTACGTTTGGTGGACC	

9. Supplementary references

[1] K. Hoshino, M. Yoshio, T. Mukai, K. Kishimoto, H. Ohno and T. Kato, *J. Polym. Sci. Part A: Polym. Chem*., 2003, **41**, 3486.

[2] D. Kuo, M. Liu, K. R. S. Kumar, K. Hamaguchi, K. P. Gan, T. Sakamoto, T. Ogawa, R. Kato, N. Miyamoto, H. Nada, M. Kimura, M. Henmi, H. Katayama and T. Kato, *Small*, 2020, **16**, 202001721.

[3] W. Zhang, X. Chen, J. Pan, C. Gao and J. Shen, *RSC Adv*., 2016, **6**, 114750.

[4] K. Hamaguchi, R. Ichikawa, S. Kajiyama, S. Torii, Y. Hayashi, J. Kumaki, H. Katayama and T. Kato, *ACS Appl. Mater. Interfaces*, 2021, **13**, 20598.

[5] S. Wolf, J. Hewitt and G. E. Greening, *Appl. Environ. Microbiol*., 2010, **76**, 1388.

[6] D. Besselsen, A. Wagner and J. Loganbill, *Comp. Med*., 2002, **52**, 111.

[7] M. Kitajima, A. Hata, T. Yamashita, E. Haramoto, H. Minagawa and H. Katayama, *Appl. Environ. Microbiol*., 2013, **79**, 3952.

[8] US Center of Disease Control, CDC's Influenza SARS-CoV-2 Multiplex Assay. https://www.cdc.gov/coronavirus/2019-ncov/lab/multiplex.html (accessed 10

February 2023)